Soils and Rocks

An International Journal of Geotechnical and Geoenvironmental Engineering

www.soilsandrocks.com

ISSN 1980-9743
ISSN-e 2675-5475

Influence of industrial effluent treatment ettringite on the compressive and tensile strength and microstructure of soil-cement mixtures

Angélica Vinci do Nascimento Gimenez Rios[1], Fernando Franco Sguarezi[1], Cláudia Telles Benatti[1], Juliana Azoia Lukiantchuki[1#]

Article

Keywords
Ettringite
Portland cement
Unconfined compressive strength
Indirect tensile strength
Microstructure

Abstract

It is increasingly important to find solutions for the problem of the aluminium anodising industry which generates a large amount of acid and alkaline wastewater, composed of high amounts of phosphates, sulphates, nitrates and aluminium. The sulphate removal trough ettringite precipitation is a simple process and involves a low-cost operating. The ettringite can be also formed during the cement hydration in soil-cement mixtures which causes several damages such as expansion. However, the effect of ettringite on the compressive strength, tensile strength and microstructure have few studies. This paper presents a novel experimental study on the influence of the industrial effluent treatment ettringite in resistance and microstructure of soil-cement mixtures. Experimental tests were performed using natural soil, soil mixed with 5% and 6% of cement and soil mixed with 5% and 6% of cement and ettringite for each material. The resistance of the materials was evaluated by unconfined compressive strength and indirect tensile strength, after 3, 7 and 14 days of cure. Additionally, several characterization tests and microstructure analysis were performed. Regarding the experimental results, the compressive strength and tensile strength decreases about 75% and 85%, respectively, when ettringite was added in soil-cement mixtures. The microstructure of natural soil, soil-cement and soil-cement-ettringite mixtures shows that the addition of cement and ettringite, simultaneously, increases the ettringite crystal formation mainly because the cement functions as a source of sulfate ions contributing with the formation of more crystals. Experimental results indicate that the incorporation of ettringite in soil-cement mixtures is not suitable for geotechnical applications.

1. Introduction

The aluminium anodising industry are linked to an industrial sector which produces great amounts of different waste streams. The aluminium is the most important material to be anodized although on a much smaller scale, magnesium, titanium, tantalum and niobium are also anodized (Álvarez-Ayuso, 2009). The anodising technique consists of an electrolytical process which improves the performance of a metallic surface (Álvarez-Ayuso, 2009; Chimenos et al., 2006; Magalhães et al., 2005) using steps of degreasing, matting, anodizing, coloring, sealing, suitable cleaning and rinsing.

As a result of the anodising process, large amounts of acid and alkaline wastewater, composed of high amounts of phosphates, sulphates, nitrates and aluminium, are generated (Chimenos et al., 2006; Álvarez-Ayuso, 2009). The impact caused by sulfate emissions into the environment is not direct since it is chemically inert, non-volatile and non-toxic. However, the discharge of high concentrations of sulfate in the environment can cause an unbalance in the natural cycle of sulfur and increases the conductivity and the potential of corrosion in the receiving waters (Benatti et al., 2009; Lens et al., 1998; Silva et al., 2002; Moret & Rubio, 2003).

The removal of the sulphate from industrial wastewater can be done through reverse osmosis, electrodialysis, nanofiltration, biological reduction, ion exchange and chemical treatment with mineral precipitation, such as ettringite (Lens et al., 1998; Silva et al., 2012). The chemical treatment with ettringite precipitation is an interesting alternative since it is a simple process and involves a low-cost operating. However, this method produces a large amount of waste and solutions to reduce or reuse this waste should be developed (INAP, 2003).

The ettringite ($Ca_6[Al(OH)_6]_2(SO_4)_3.26H_2O$) occurs as a natural mineral or as a hydration product of Portland cement formed from the reaction of calcium and alumina, which are available in cementitious matrices, with sulfate either inherently present in the cement paste or introduced into the system through an outside source (Chrysochoou

---

[#]Corresponding author. E-mail address: jalukiantchuki@uem.br
[1]Universidade Estadual de Maringá, Departamento de Engenharia Civil, Maringá, PR, Brasil.

Submitted on January 30, 2023; Final Acceptance on January 22, 2024; Discussion open until May 31, 2024.
https://doi.org/10.28927/SR.2024.001023

& Dermatas, 2006). The ettringite formation frequently is associated with expansion and deterioration of concrete structures associated with sulphate attack (Mehta, 1973; Diamond, 1996). However, no ettringite-related expansion necessarily produces damaging disruption of concrete structures (Collepardi, 2003).

The ettringite formation in chemical-soil stabilization is associated with high concentration of sulphates and low concentration of silica which is precipitated on the solid clay particles (Mitchell, 1986; Wild et al., 1993, 1999; Puppala et al., 2004; Li et al., 2020). The colloidal gel, formed from ettringite crystallization, has the ability of attracting water molecules and, consequently, creating inter-particles repulsion and system expansion (Wild et al., 1999). Several studies reported issues associated with the expansion induced by the formation and hydration of ettringite mineral in natural soils with high concentration of sulphates treated with lime and cement (Mitchell, 1986; Perrin, 1992; Puppala et al., 1999, 2005).

The understanding of ettringite formation in soil-cement or soil-lime mixture is still very complex, but the impact of expansion in geotechnical applications is well discussed. Ebailila et al. (2022) evaluated the suitability to suppress the ettringite induced expansion using lime and silica-fume at varying dosages of 4%, 6% and 10%. Results show that the silica fume is suitable for restricting the ettringite formation and suppressing the expansion when combined with 3% of lime and 7% of silica-fume. Additionally, Wild et al. (1999) used ground granulated blastfurnace slag (GGBS), an industrial by-product, to suppress the expansion of a clay soil stabilized with lime in the presence of gypsum. The experimental results show that replacing lime with GGBS reduces the linear expansion of soil-lime mixtures, mainly in the presence of gypsum. The ettringite induced expansion also can be controlled using a liquid ionic stabilizer, geopolymers based on metakaolin and fly ash, and a nanotechnology-based product, composed of synthetic zeolite, alkaline metals, and some activators (He et al., 2018; Khadka et al., 2020; Eyo et al., 2021).

However, the ettringite synthesized in laboratory and mixed with soils does not present the similar behavior of the ettringite formed during chemical soil stabilization. Experimental results, presented by Puppala et al. (2005), show that the synthesized ettringite swelling is smaller than the soil specimens without ettringite. The difference can be attributed to the strengthening reactions of the ettringite to the soils and the low moisture adsorption capacities of the compacted and hydrated ettringite minerals.

This research presents a novel study on the incorporation of industrial effluent treatment ettringite in the compressive, tensile strength and microstructure of soil-cement mixtures and the natural soil. The effect of ettringite incorporation was evaluated by varying the ettringite, the soil and cement contents and the curing time. Despite numerous studies on ettringite expansion, few ones have evaluated the influence of the ettringite on the resistance of the soil-cement mixtures and the natural soil.

2. Materials and methods

2.1 Materials

The soil selected for this study is a typical Brazilian lateritic soil, since this type of material covers 70% of national territory (Medina & Motta, 2015). The soil was collected in a site located in the city of Mandaguaçu, in the northern region of Parana state, Brazil. According to the MCT (Miniature, Compacted, Tropical) method, the soil was classified as lateritic clayey sand - LA (Nogami & Villibor, 1991). This lateritic soil is from a basalt residual clayey sand and composed of fine sandstone. Further information about the soil properties can be obtained in previous research (Lukiantchuki et al., 2021). The samples were dried until reaching hygroscopic water content. Afterwards, the samples were sieved in a #2.0 mm sieve and stored in containers.

The selected Portland cement was CP-II-Z-32 which is predominantly composed of clinker and contains calcium sulphates and pozzolanic materials (6-14%). The chemical composition is around 53% and 23% of calcium oxide (CaO) and silica (SiO_2), respectively. Other chemical components are aluminium oxide (AL_2O_3) 8%, sulfur trioxide (SO_3) 5%, ferric oxide (Fe_2O_3) 6% and magnesium oxide (MgO) 3%.

The wastewater used to produce the ettringite was collected in an aluminium anodising plant located in the city of Maringá, Paraná state, Brazil. The ettringite was produced at the Laboratory of Environmental Sanitation at the State University of Maringá (UEM) from two different materials: a) raw wastewater and b) pre-treated wastewater.

Preliminary analysis shows that high acidity in the raw wastewater contributes with the dissolution of calcium hydroxide and consequently the *pH* increase providing calcium ions for ettringite molecules. Therefore, a post-treatment might be necessary to reach the suitable wastewater discharging parameters. For the pre-treated wastewater (neutral *pH*), it is necessary to use a more soluble salt (dehydrated calcium chloride) which increases the cost of this procedure. The pre-treated wastewater was adopted in this study since results show that the use of pre-treated wastewater did not change the characteristics of the ettringite produced, allowing production in a large scale and in an effective way.

The ettringite was produced though a chemical precipitation process presented by Santos et al. (2019). The process of production consists of: a) check the *pH* of pre-treated wastewater to confirm alkaline condition; b) measure the sulphate concentration through a turbidimeter; c) define the dosage of dehydrated calcium chloride and aluminium hydroxide through a stoichiometric analysis; d) add the reagents to the pre-treated wastewater (Figure 1a); e) process of decantation of the precipitate for 48 hours; f) removal of the supernatant and drying of the precipitate product (ettringite); g) ettringite drying, crushing, sieving in

(a) Wastewater during agitation (Jar test)

(b) Ettringite (dried and crushed)

Figure 1. Process of ettringite production from pre-treated wastewater.

a #2.0 mm sieve and storing in containers for geotechnical tests (Figure 1b).

2.2 Methods

The methodology used in this research is based on the following steps: a) physical, chemical and mineralogical characterization of the materials; b) mechanical strength tests; and c) morphological analyses of the materials.

2.2.1 Chemical, physical, and mineralogical characterization

The chemical, physical and mineralogical characterization of the materials was conducted through the following tests: particle size distribution (PSD) (ASTM, 2017a), particle size distribution by laser diffraction for cement and ettringite, particle density of the soil (ASTM, 2014), Atterberg limits tests (ASTM, 2017b), *pH* tests (ASTM, 2001), standard effort compaction tests (ASTM, 2012), X-ray diffraction -XDR, ettringite pozzolanic activity (ABNT, 2010). Moreover, the organic matter (Teixeira et al., 2017) and cation exchange capacity (*CEC*) (Teixeira et al., 2017) tests were also performed.

The particle size distribution (PSD) by laser diffraction is suitable for very fine particles materials. The PSD tests were carried out in samples diluted in alcohol using a Mastersizer 2000 (Malvern), which can identify particles ranging from 0.02 to 2000 μm.

The XDR mineralogical analyses were performed on the soil, cement and ettringite samples, which were prepared using a 0.075 mm sieve. Tests were conducted using a Shimadzu diffractometer with CuKα radiation over a 2θ angular range of 3.0°-70°, with 1 s/step (0.02°).

2.2.2 Physicochemical tests

The evaluation of chemical stabilization of the soil was carried out using the physicochemical method proposed by Chadda (1971). The method is based on the electrical interaction between cement and clayey soil particles, which promotes physicochemical changes in the soil-cement mixtures associated with volumetric variations. The physicochemical tests were carried out using mixtures of soil-cement and soil-cement-ettringite with different contents of cement and ettringite. The sample cement content that presents the highest volumetric variation indicates the stability of the mixture, defined as the minimum cement content required for the soil to stabilize (Chadda, 1971).

Table 1. Sample characteristics adopted for mechanical tests.

Materials	*S* (%)	*C* (%)	*E* (%)
S	100	-	-
SC$_5$	95	5	-
SC$_6$	94	6	-
SE$_5$	95	-	5
SE$_6$	94	-	6
SC$_5$E$_5$	90	5	5
SC$_6$E$_6$	88	6	6

Legend: see List of Symbols.

2.2.3 Molding and cure of the specimens

The compaction tests were carried out to assess the optimum water content (w_{op}) and the maximum dry unit weight (γ_{dmax}) for the studied materials. Proctor compaction tests were performed using Brazilian standard effort (600 kJ/m^3). Table 1 presents the proportion of materials for each mixture which was calculated based on the dry mass of the soil. The materials were mixed by hand until reaching homogeneous aspect. Then, distilled water was added to reach the target water content followed by the material compaction.

Regarding the mechanical tests, five cylindrical specimens, one for each specific situation, were molded using the previously obtained compaction parameters (w_{op} and γ_{dmax}). The specimens were molded in five layers and had diameter and height of 50 and 100 mm, respectively. The specimens with cement and ettringite were wrapped in waterproof plastic and stored in a wet room to cure for 3, 7 and 14 days before testing. The wet room maintains a humidity value higher than 95% and a temperature between 21.0-25.0 °C. Natural soil specimens were not subjected to a cure procedure.

The specimens were submerged in water for 24 hours before reaching the pre-established curing period. This procedure was necessary because the specimens were in unsaturated conditions and therefore could present suction effect. Thus, to increase the saturation of the specimens and decrease the influence of suction on strength measures, it was adopted a 24 hours of water submersion (Consoli et al., 2007; Lukiantchuki et al., 2021). After submersion, the mass and the water content of the specimens were measured, and the strength tests were performed.

2.2.4 Mechanical strength tests

The mechanical performance of the materials was evaluated using the unconfined compressive strength test (*UCS*) (ASTM, 2016a) and the indirect tensile strength (*ITS*) (ASTM, 2016b) test. As acceptance criteria for the *UCS* and *ITS* values, at least five specimens, molded in the same conditions, had to show the same results within a 12% variation from the mean.

2.2.5 Scanning electron microscopy (SEM)

The SEM tests were carried out in the compacted specimens after 7 days of curing using Shimadzu Superscan (SS-550) microscope, operating with an acceleration voltage of 10 kV, with a magnification capacity of 20 to 300,000 times. For the tests, small pieces of the specimens were fixed on carbon tape and coated with a conductive material.

3. Results and discussion

3.1 Material characteristics

The properties of the natural soil are presented in Table 2 and the particle size distribution of the materials is shown in Figure 2. Results show that the natural soil presents a very low organic matter (*OM*) content, which is suitable for chemical soil-cement stabilization. The organic matter reacts with hydration products, resulting in low *pH* values which may retard the hydration process (Makusa, 2012). The cation exchange capacity results are also very low which indicates the presence of clay minerals from the kaolinite group, as mentioned in previous research (Lukiantchuki et al., 2021). The presence of iron (Fe) is expected since the soils of the region are classified as lateritic thus showing in their composition the presence of iron and aluminium oxides. Additionally, the soil presents an acid *pH* as reported in previous research (Ladeira & Sandoli, 2019) as well as specific gravity of 2.63, similar to expected value of the quartz, a mineral present in sandy soils. The sulfate content of the natural soil is about 45.7 mg/kg, a very low value when compared to other studies where the ettringite formation occurs in soils with 233 mg/kg to 43500 mg/kg of sulfate content (Puppala et al., 2005).

Figure 2 shows the comparison between the particle size distributions of the soil, the cement and the ettringite. The soil has a granulometric distribution of 73% of sand, 22% of clay and 5% of silt, therefore classified as clayey sand. The particle size classification of cement and ettringite was based on Christofoletti & Moreno (2017) approach to Udden-Wentworth proposal. The PSD curve for the ettringite shows the predominance of particles between 10-100 µm

Table 2. Properties of the soil.

Parameter	Value
Gravel content (%)	0
Sand content (%)	73
Silt content (%)	5
Clay content (%)	22
w_L (%)	25
PI (%)	12
Un. Soil Classif. System (USCS)	SC
pH (KCl)	3.9
pH (H_2O)	4.2
pH ($CaCl_2$)	3.8
OM (%)	0.35
CEC ($cmol_c$/Kg)	3.59
Fe (mg/dm^3)	50.34
Sulfate content (mg/kg)	45.7
Specific gravity (g/cm^3)	2.63

Legend: see List of Symbols.

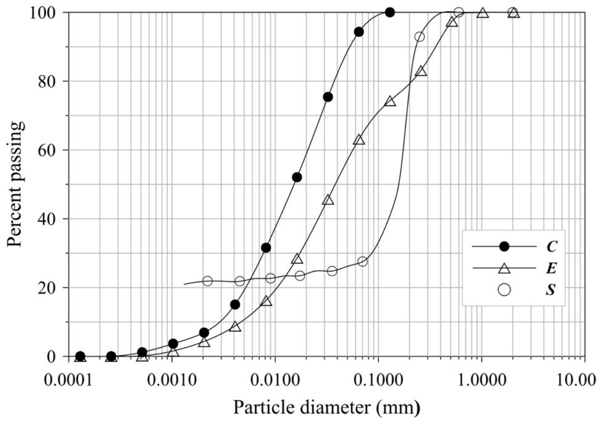

Figure 2. Particle size distribution (PSD) curves.

(53%) classified as fine siltstone to very fine sandstone. For the Portland cement, a predominance of particles between 10-100 µm (61%) was also observed. Moreover, it was observed that the Portland cement has a higher percentage of particles in the range of 1-10 µm when compared to ettringite, while ettringite has a higher percentage of particles in the range of 100-1000 µm when compared to cement.

The pozzolanic activity of the ettringite shows a consumption of 174 mg of calcium hydroxide ($Ca\ (OH)_2$). According to NBR 15895 (ABNT, 2010), additions incorporated into the Portland cement composition may be considered pozzolan when the consumption is greater than 436 mg ($Ca\ (OH)_2$)/g. The calcium hydroxide consumption values were lower than the minimum limit established in the standard. The pozzolanic reaction capability is useful information since it converts the relatively soluble calcium hydroxide into C-S-H which increases strength and reduces the permeability of the material (Artuso & Lukiantchuki, 2019).

The X-ray diffraction (XDR) mineralogical analysis indicates that the soil is composed of feldspar and quartz. Additionally, the presence of kaolinite and halloysite was observed, which are clay minerals of low cation-exchange capacity and typical of lateritic soils. The analysis detected the presence of magnetite, iron oxide hematite and alumina, which are associated with the laterization process.

Regarding the cement, the XDR analyses detected primary minerals such as muscovite, gypsum, alumina, quartz, anhydrite, among others. The cement is composed of lime (CaO), silica (SiO_2), alumina (AL_2O_3), iron oxide (Fe_2O_3), magnesia (MgO), alkalis (Na_2O and K_2O) and sulfates (SO_3). The presence of muscovite is frequently detected in Portland cement. The muscovite occurs in magmatic rocks, metamorphic and sedimentary rocks.

Concerning the ettringite, the XDR analyses detected the presence of ettringite mineral, anhydrite, hydrated calcium silicate (laumontite) and portlandite. The ettringite is a calcium sulfate and hydrated aluminum composed mineral, which justifies the presence of hydrated calcium silicate and portlandite. The anhydrite has a composition associated with the presence of sulfate calcium and therefore can be present in the ettringite composition.

3.2 Soil plasticity

The influence of the incorporation of cement and ettringite on the soil plasticity is presented in Table 3 and the results show that the cement or ettringite addition decreases the liquid limit (w_L) of the natural soil. Moreover, the decrease of w_L is slightly higher when ettringite is involved. The plastic limit (w_P) shows a small increase when cement is added and a small decrease when ettringite is added. Changes in plasticity occur since the incorporation of cement and ettringite modify the particle size distribution as can be presumed when granulometric curves are compared (Figure 2). The plasticity index (*PI*) decreases about 33% for all incorporations to the natural soil.

The plasticity limit test did not reach the criteria established in the standard (cylinder cracking) for specimens with ettringite. The test was interrupted when water loss was observed in a cylinder molded with a smaller diameter than the reference.

3.3 Physicochemical tests

The physicochemical tests for the soil-cement (SC) mixtures were performed in duplicate and the results are presented in Figure 3, where the maximum volumetric variation corresponds to the minimum cement content for chemical stabilization of the soil. Therefore, for this specific soil, the required amount of cement is about 6%. The results also show that for 12% cement content, the volumetric variation was similar to the one observed for 6%. However, as for 8% and 10% cement content, the volumetric variation decreased. Therefore, it is more suitable to establish an amount of 6% of cement. A previous study obtained a similar value for the minimum cement content (Ladeira & Sandoli, 2019).

The physicochemical curves for the soil-cement-ettringite (SCE) mixtures are presented in Figure 4. The tests were done in duplicate (Curve 1 and Curve 2) using 50% of each material (cement and ettringite) to evaluate the influence

Table 3. Atterberg limits results.

Materials	w_L (%)	w_P (%)	*PI* (%)
S	25	13	12
SC_5	22	14	8
SC_6	23	15	8
SE_5	20	12	8
SE_6	20	12	8
SC_5E_5	21	13	8
SC_6E_6	21	13	8

Legend: see List of Symbols.

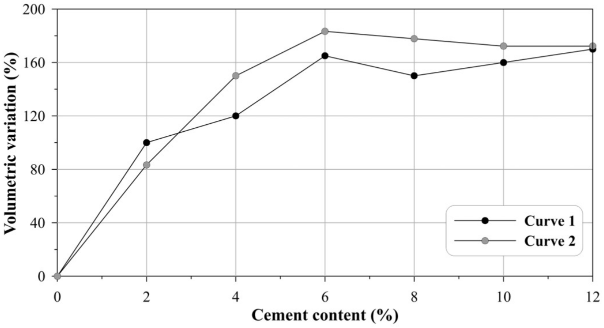

Figure 3. Volumetric variation versus cement content for soil-cement mixtures.

Table 4. *pH* results.

	S	SC_6	SE_6	SC_6E_6
pH (H_2O)	4.9	12.1	7.1	11.6
pH (KCl)	4.2	12.2	7.0	11.5
ΔpH	-0.7	0.1	-0.1	-0.1
PZC	3.5	12.3	6.9	11.4

Legend: see List of Symbols.

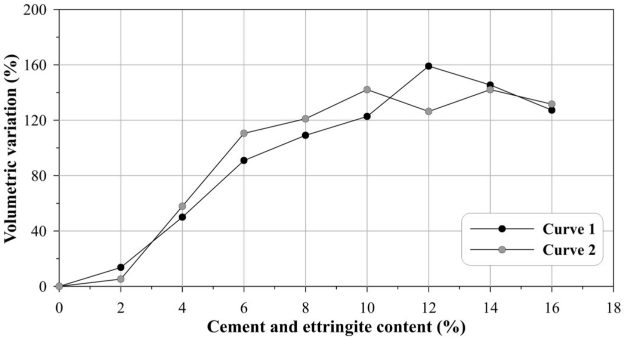

Figure 4. Volumetric variation versus cement and ettringite content for soil-cement-ettringite mixtures.

Table 5. Estimated compaction parameters.

Materials	γ_{dmax} (kN/.m^{-3})	w_{op} (%)
S	19.22	12.00
SC_5	19.38	12.15
SC_6	19.25	12.70
SE_5	19.50	11.20
SE_6	19.50	11.50
SC_5E_5	19.46	11.50
SC_6E_6	19.52	11.50

Legend: see List of Symbols.

of ettringite in the stabilization of soil-cement mixtures. The results show that, for 10% (Curve 2) and 12% (Curve 1) of cement-ettringite content, the chemical stabilization of the soil can be reached, which corresponds to 5% - 6% of cement and 5% - 6% of ettringite.

The results show that the minimum cement content for soil-stabilization is not related with the amount of ettringite since the values for soil-cement and soil-cement-ettringite were very similar. Therefore, the physicochemical tests did not indicate the influence of ettringite in soil-chemical stabilization.

3.4 *pH*

Table 4 presents the *pH* average values obtained during 0.5, 1, 24 and 72 hours. The *pH* values did not present a significant variation and the average values were adopted. The results show that the natural soil has an acid behavior. However, the soil-cement mixture presented an alkaline behavior when cement was added. Despite the *pH* increase associated with the addition of the ettringite into to the natural soil, the soil-ettringite mixture presented a neutral behavior. The soil-cement-ettringite mixture also presented an alkaline behavior. The ΔpH was estimated using the Equation 1:

$$\Delta pH = pH\left(H_2\mathrm{O}\right) - pH\left(\mathrm{KCl}\right) \quad (1)$$

Mengue et al. (2017) evaluated the physicochemical characteristics of soil-cement mixed with a lateritic soil at a different content. The authors found a significant *pH* increase between 0% and 6% of cement and a very slightly increase between 6% and 9% of cement. The results show that an amount of 6% of cement is required to a suitable environment for cement hydrate products formation. The alkaline environment contributes with the hydration cement reactions development and consequently a better mechanical behavior can be expected. Additionally, Wang & Siu (2006) showed that higher *pH* values convert positive charges to negative ones providing a flocculated soil-cement mixture and as consequence a packed structure is formed.

The point of zero charge (*PZC*) corresponds to the *pH* value when negative charges and positive charges are equal and the ΔpH negative values indicate the predominance of negative charges. Therefore, the results presented in Table 4 show that the natural soil, soil-ettringite mixture and soil-cement-ettringite mixture tend to retain more cations than anions unlike the soil-cement mixture.

3.5 Compaction curves

The compaction parameters estimated for the mixtures are shown in Table 5 and the results show that the cement and ettringite additions cause a slight increase in the maximum dry unit weight. Also, the optimum water content increases and decreases with cement and ettringite additions, respectively. The colloidal gel formed during the ettringite crystallization attracts water molecules (Wild et al., 1999) and consequently the hydration process of the ettringite consumes a large amount of water. Compaction tests were

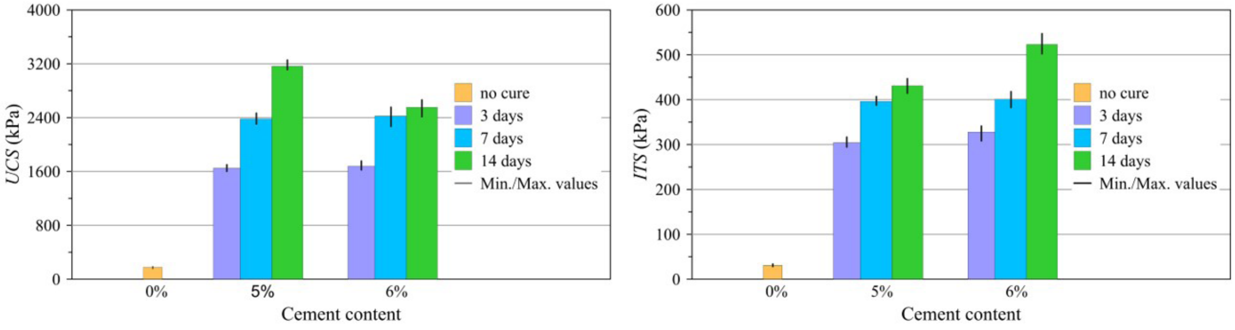

(a) *UCS* (kPa) (b) *ITS* (kPa)

Figure 5. Average values of *UCS* and *ITS* for different cement content as function of curing time.

conducted immediately after adding water and therefore the hydration of the ettringite may not have been complete. To confirm this behavior, further tests are recommended in which the mixtures should be sealed in plastic bags and left to hydrated for at least 24 h prior to compaction.

Additionally, the results show that the compaction parameters for soil-cement-ettringite mixtures present similar values than those for soil-ettringite mixtures. Thus, the compaction parameters behavior is more influenced by the ettringite than the cement.

3.6 Influence of cement incorporation on the *UCS*, *ITS* and microstructure of the natural soil

The first analysis was to evaluate the influence of the cement incorporation on the unconfined compressive strength and indirect tensile strength. The *UCS* and *ITS* average values, for different cement contents and curing times, are presented in Figure 5. As expected, the results show that the cement addition significantly increases the *UCS* and *ITS* of the natural soil. For this specific study, the *UCS* results did not indicate a significant influence when a 14 days cure mixture with 5% or 6% of cement was tested. Furthermore, the specimens with 6% of cement showed lower resistance than the specimens with 5% of cement. However, the *ITS* of the natural soil increased with the increase in the cement content and curing time.

The normalized values of *UCS* (N_{UCS}) and *ITS* (N_{ITS}), presented in Figure 6, correspond to the *UCS* or *ITS* values of the soil-cement mixture divided by the *UCS* or *ITS* of the natural soil. Results show that the incorporation of 5% to 6% of cement increases from 3 to 18 times the *UCS* of natural soil. Results also show that the resistance increases as the curing time increases. An exception was observed for SC$_6$ after 14 days of curing time, which presented a similar *UCS* value of SC$_6$ after 7 days of curing time. For this specific situation, the delayed ettringite formation should be investigated. Regarding the *ITS*, the results show that, for 3 and 7 days of curing time, the samples with 5% or 6% of cement did not show significant difference while, for 14 days of curing time, the use of 6% of cement improves the *ITS* strength in 20% when compared to the use of 5% of cement.

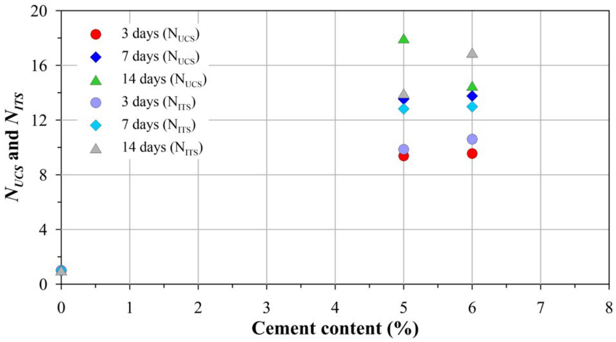

Figure 6. Normalized values of *UCS* and *ITS* for soil-cement mixtures.

The improvement due to incorporation of cement on *UCS* and *ITS* was expected and reported in several studies in the literature (Fonseca et al., 2009; Consoli et al., 2012; Portelinha et al., 2012; Lukiantchuki et al., 2021). Figure 7 presents the micrograph of natural soil and soil-cement mixture with 6% of cement, respectively. Figure 7a shows the presence of pores (voids) and materials with plate or lamellar shape (clay minerals), very similar to the kaolinite mineral. Considering the characterization results and the lateritic classification of the soil, it could be identified as kaolinite. Figure 7b shows the soil-cement structure, where ettringite crystals formed from cement hydration can be identified. Moreover, the impregnation of cement particles on the surface of the grains is evident.

3.7 Influence of ettringite incorporation on the *UCS*, *ITS* and microstructure of natural soil

The *UCS* and *ITS* average values, for different ettringite contents and curing times, are presented in Figure 8. Results show that the ettringite incorporation to the natural soil did not significantly affect the resistance when compared with the Portland cement incorporation. Results also show that the *UCS* and *ITS* did not increase

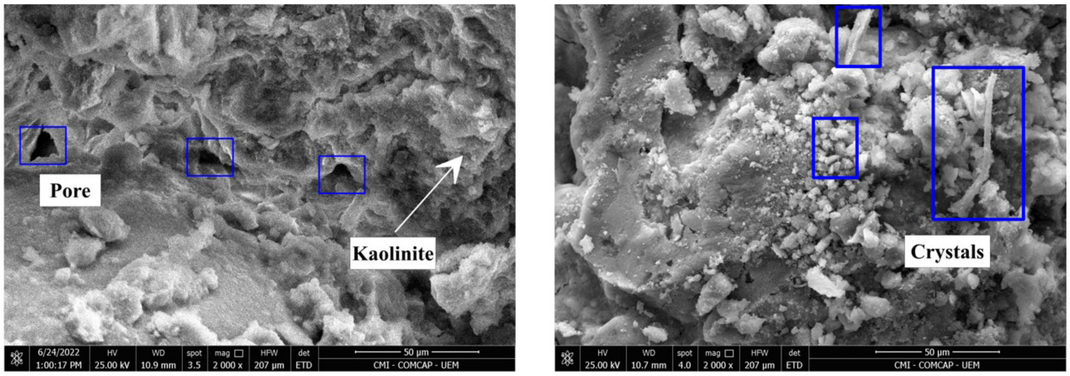

(a) Natural soil - 2000X **(b) SC_6 - 2000X**

Figure 7. Scanning electron micrograph: (a) natural soil (S) and (b) soil-cement mixture (SC_6).

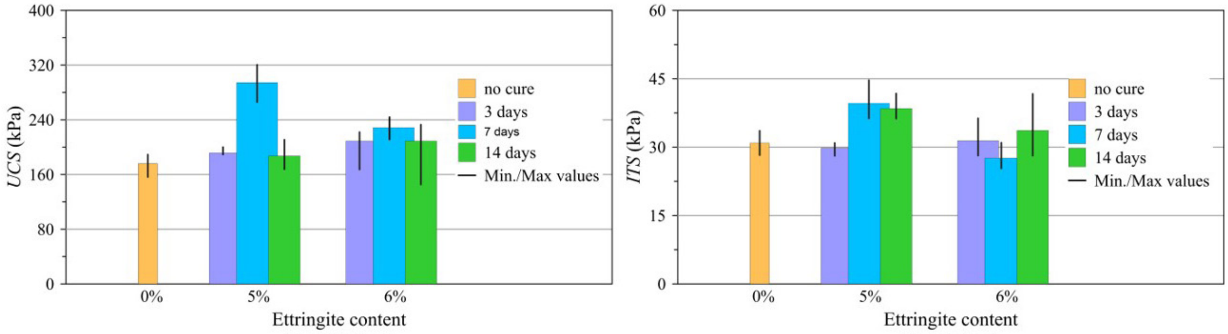

(a) *UCS* (kPa) (b) *ITS* (kPa)

Figure 8. Average values of *UCS* and *ITS* for different ettringite content as function of curing time.

over time and no pozzolanic behavior of the ettringite can be confirmed.

The influence of ettringite incorporation on *UCS* and *ITS* can be seen in Figure 9, where the *UCS* normalized values are between 1 to 1.64 times the natural soil *UCS* ones and the *ITS* normalized values are between 0.89 to 1.28 times the natural soil *ITS* ones. The highest *UCS* and *ITS* values were for SE_5 with 7days of cure, while for 6% of ettringite, the *ITS* results decrease or remains similar to the natural soil. However, despite the experimental results indicate that the incorporation of ettringite does not affect the soil resistance, the expansion of the soil-ettringite mixture should be evaluated. The soil-ettringite mixture micrograph (Figure 10) shows that the ettringite incorporation causes crystals formation, which is not observed in natural soil (Figure 7a). Ettringite crystals have a similar size to that presented by Taylor et al. (2001) and a random orientation. The ettringite incorporation to the soil consists of calcium sulfate and hydrated aluminum addition, which causes crystals formation and can lead to an increase in material volume and therefore expansion.

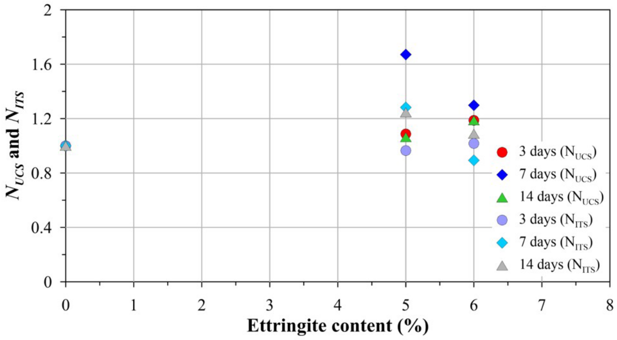

Figure 9. Normalized values of *UCS* and *ITS* for soil-ettringite mixtures.

3.8 Influence of cement and ettringite incorporation on the *UCS*, *ITS* and microstructure of natural soil

The unconfined compressive strength and tensile strength values for soil-cement-ettringite mixtures (SC_5E_5 and SC_6E_6) show that the incorporation of ettringite in soil-cement mixtures impaired the performance of the cement since the cement works as a source of sulfate ions contributing to the formation of more ettringite crystals. The comparison between Figure 5 and Figure 11 shows a very significant decrease in *UCS* (75%) and *ITS* (85%) when ettringite was added to soil-cement mixtures. Results also show that the strength values decrease as the cement content increases.

The Figure 12 shows the *UCS* and *ITS* normalized values for soil-cement-ettringite mixtures, where the incorporation of ettringite in soil-cement mixtures increases the resistance of natural soil (Figure 11) but the values were significantly lower than the values observed for soil-cement mixtures (Figure 6). The addition of ettringite simultaneously to the cement impairs the performance of the material, inhibiting the potential of the Portland cement and consequently preventing the mixtures from gaining strength.

The experimental results indicate that the incorporation of ettringite, obtained from industrial effluent treatment, causes a negative impact on the compressive and tensile strength of soil-cement mixtures. The ettringite is a calcium aluminium sulfate mineral and during the colloidal gel formed in crystallization, the mineral attracts water molecules while the clay soil particles are repulsed by them, thus leading to a system expansion (Wild et al., 1999). A possible explanation for the strength decrease is the absence of cement hydration products, which are responsible for the cement paste hardening. As the ettringite attracts water molecules, the cement hydration process is compromised.

The soil-cement-ettringite microstructure, presented in Figure 13, indicates that the dominant presence of ettringite crystals adhered to each other and filled a great volume of the matrix. The addition of cement and ettringite, simultaneously, increases the crystal formation and the cement serves as a source of sulfate ions contributing with the formation of more ettringite crystals.

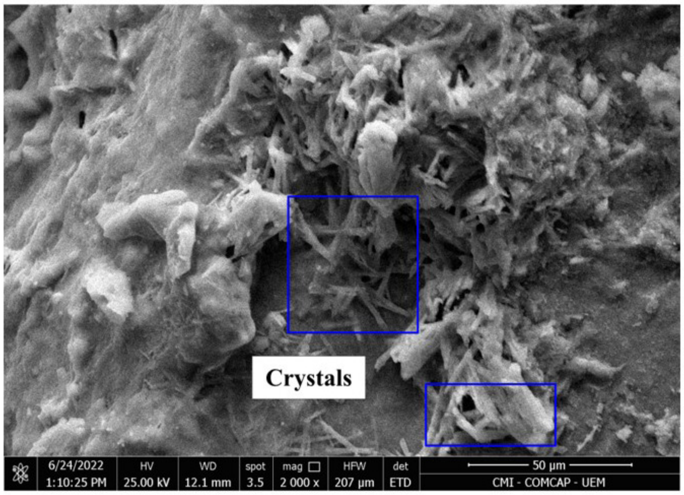

SE_6 - 2000X

Figure 10. Scanning electron micrograph of soil-ettringite mixture (SE_6).

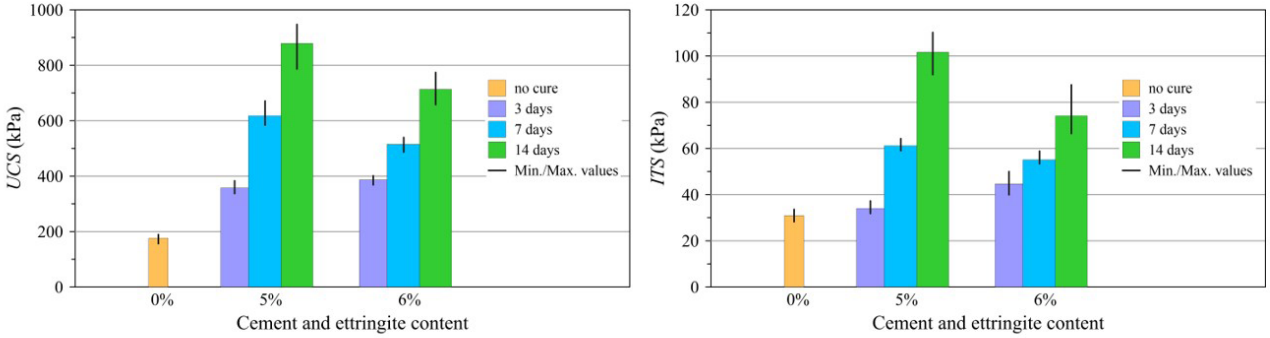

(a) *UCS* (kPa)

(b) *ITS* (kPa)

Figure 11. Average values of *UCS* and *ITS* for different cement and ettringite content as function of curing time.

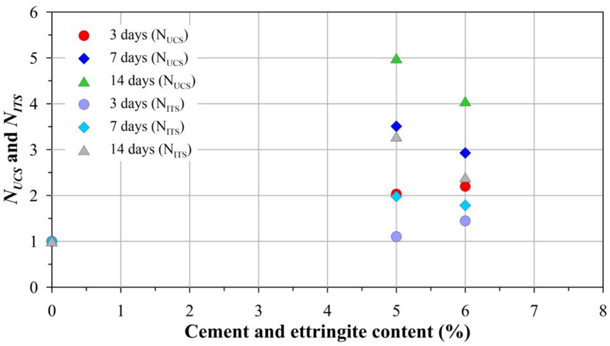

Figure 12. Normalized values of *UCS* and *ITS* for soil-cement-ettringite mixtures.

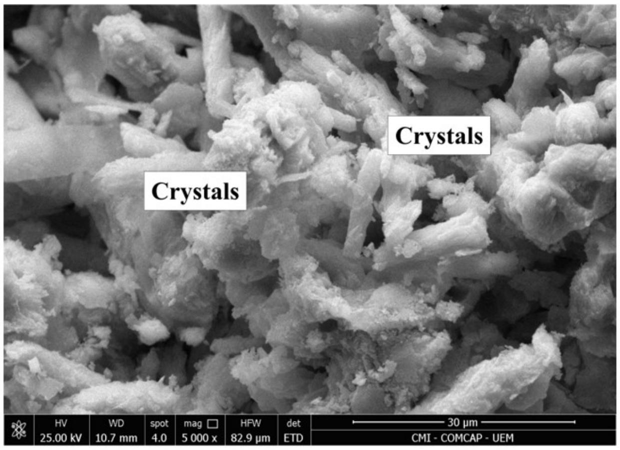

SC_6E_6 - 2000X

Figure 13. Scanning electron micrograph of soil-cement-ettringite mixture (SC_6E_6).

4. Conclusion

Ettringite samples produced from the removal of the sulphate aluminium in the wastewater of anodising industry was incorporated in a natural lateritic soil and soil-cement mixtures to evaluate its effect on the compressive strength, tensile strength, and microstructure. Results show that the ettringite has very fine particles, as Portland cement, and does not present pozzolanic characteristics. The characterization tests show that when ettringite and cement were mixed with natural soil, the plasticity index decreases and the *pH* value increases. The physicochemical tests show that the minimum cement content for soil-cement stabilization is independent on the ettringite amount since the values for soil-cement and soil-cement-ettringite are similar. Additionally, the compaction results show that the cement and ettringite additions cause a slight increase in the maximum dry unit weight. Also, the optimum water content increases and decreases with cement and ettringite additions, respectively. Regarding the compressive and tensile strength, results show that ettringite does not significantly change the soil resistance. However, when the ettringite is added simultaneously with the cement, it impairs the performance of the material, inhibiting the potential of hydration reactions and consequently preventing the mixtures from gaining strength. The ettringite attracts the water molecules and the hydration process of Portland cement is impaired. The microstructure of natural soil, soil-cement and soil-cement-ettringite mixtures shows that the addition of cement and ettringite, simultaneously, increases the ettringite crystal formation mainly because the cement works as a source of sulfate ions contributing to the formation of more ettringite crystals. Regarding the compressive and tensile strength, this study shows that the presence of ettringite in soil-cement mixtures is not suitable for geotechnical applications. However, further analyses considering other types of cement and longer hydration times for ettringite must be considered.

Acknowledgements

The authors thank the scholarship received from CAPES (Coordination for the Improvement of Higher Education Personnel). Authors also thank the Laboratory of Soil Mechanics and the Laboratory of Environmental Sanitation at the State University of Maringa (UEM). Furthermore, the authors appreciate the helpful corrections and suggestions of this paper reviewers.

Declaration of interest

The authors have no conflicts of interest to declare. All co-authors have observed and affirmed the contents of the paper and there is no financial interest to report.

Authors' contributions

Angélica Vinci do Nascimento Gimenez Rios: investigation, data curation, writing – original draft. Fernando Franco Sguarezi: investigation, data curation, validation. Cláudia Telles Benatti: conceptualization, methodology, supervision, revision. Juliana Azoia Lukiantchuki: conceptualization, methodology, supervision, writing, revision.

Data availability

The datasets generated and analyzed in the course of the current study are available from the corresponding author upon request.

List of symbols and abbreviations

pH	potential of hydrogen
pH ($CaCl_2$)	potential of hydrogen in calcium chloride

pH (H_2O)	potential of hydrogen in water
pH (KCl)	potential of hydrogen in potassium chloride
w_L	liquid limit
w_{op}	optimum water content
w_P	plastic limit
AL_2O_3	aluminium oxide
C	cement
CaO	calcium oxide
$Ca(OH)_2$	calcium hydroxide
CEC	cation exchange capacity
CP-II-Z-32	Portland cement
C-S-H	calcium silicate hydrate
E	ettringite
Fe	iron
Fe_2O_3	ferric oxide
G_s	specific gravity
ITS	indirect tensile strength
K_2O	alkalis
LA	lateritic clayey sand
MCT	miniature, compacted, tropical
MgO	magnesium oxide
Na_2O	alkalis
N_{ITS}	normalized values of *ITS*
N_{UCS}	normalized values of *UCS*
OM	organic matter
PI	plasticity index
PSD	particle size distribution
PZC	point of zero charge
S	natural soil
SC	soil-cement mixture
SC	clayey sand
SC_5	sample with 5% of cement (dry weight basis)
SC_6	sample with 6% of cement (dry weight basis)
SCE	soil-cement-ettringite mixture
SC_5E_5	sample with 5% of cement and 5% of ettringite (dry weight basis)
SC_6E_6	sample with 6% of cement and 6% of ettringite (dry weight basis)
SE_5	sample with 5% of ettringite (dry weight basis)
SE_6	sample with 6% of ettringite (dry weight basis)
SEM	scanning electron microscopy
SiO_2	silica
SO_3	sulfur trioxide
UCS	unconfined compressive strength
UEM	State University of Maringá
USCS	Unified Soil Classification System
XDR	X-ray diffraction
γ_{dmax}	maximum dry unit weight
ΔpH	delta potential of hydrogen

References

ABNT NBR 15895. (2010). *Pozzolanic materials – Determination of calcium hydroxide fixed – Modified Chapelle's method.* Associação Brasileira de Normas Técnicas, Rio de Janeiro, RJ (in Portuguese).

Álvarez-Ayuso, E. (2009). Approaches for the treatment of waste streams of the aluminium anodising industry. *Journal of Hazardous Materials*, 164(2-3), 409-414. http://dx.doi.org/10.1016/j.jhazmat.2008.08.054.

ASTM D4972-01. (2001). *Standard test method for pH of soils.* ASTM International, West Conshohocken, PA.

ASTM D698-12e12. (2012). *Standard test methods for laboratory compaction characteristics of soil using standard effort (12 400 ft-lbf/ft^3 (600 kN-m/m^3)).* ASTM International, West Conshohocken, PA. https://doi.org/10.1520/D0698-12E01.1.

ASTM D854-14. (2014). *Standard test methods for specific gravity of soil solids by water pycnometer.* ASTM International, West Conshohocken, PA. https://doi.org/10.1520/D0854-10.2.

ASTM D2166. (2016a). *Standard test method for unconfined compressive strength of cohesive soil.* ASTM International, West Conshohocken, PA. http://dx.doi.org/10.1520/D2166_D2166M-16.

ASTM D3967. (2016b). *Standard test method for splitting tensile strength of intact rock core specimens.* ASTM International, West Conshohocken, PA. http://dx.doi.org/10.1520/D3967-16.

ASTM D7928-17. (2017a). *Standard test method for particle-size distribution (gradation) of fine-grained soils using the sedimentation (hydrometer) analysis.* ASTM International, West Conshohocken, PA. http://dx.doi.org/10.1520/D7928-17.

ASTM D4318-17e1. (2017b). *Standard test methods for liquid limit, plastic limit, and plasticity index of soils* (Vol. 4, pp. 1-14). ASTM International, West Conshohocken, PA. http://dx.doi.org/10.1520/D4318-10.

Artuso, F., & Lukiantchuki, J.A. (2019). Evaluation of the self-cemeting effect of Construction and Demotion Waste (CDW) on mechanical performance over time for pavement support layers purpose. *Ambiente Construído*, 19(2), 59-77. http://dx.doi.org/10.1590/s1678-86212019000200308.

Benatti, C.T., Tavares, C.R.G., & Lenzi, E. (2009). Sulfate removal from waste chemicals by precipitation. *Journal of Environmental Management*, 90(1), 504-511. http://dx.doi.org/10.1016/j.jenvman.2007.12.006.

Chadda, L.R. (1971). A rapid method of assessing the cement requirement for the stabilization of soils. *Indian Concrete Journal*, 45(7), 298-314.

Chimenos, J.M., Fernández, A.I., Hernández, A., Haurie, L., Espiell, F., & Ayora, C. (2006). Optimization of phosphate removal in anodizing aluminium wastewater. *Water Research*, 40(1), 137-143. http://dx.doi.org/10.1016/j.watres.2005.10.033.

Christofoletti, S.R., & Moreno, M.M.T. (2017). Granulometria por difração a laser e sua relação com a faciologia das rochas argilosas da Formação Corumbataí – SP. *Cerâmica*, 63(367), 303-310. http://dx.doi.org/10.1590/0366-69132017633672096.

Chrysochoou, M., & Dermatas, D. (2006). Evaluation of ettringite and hydrocalumite formation for heavy metal immobilization: literature review and experimental study. *Journal of Hazardous Materials*, 136(1), 20-33. http://dx.doi.org/10.1016/j.jhazmat.2005.11.008.

Collepardi, M. (2003). A state-of-the-art review on delayed ettringite attack on concrete. *Cement and Concrete Composites*, 25(4-5), 401-407. http://dx.doi.org/10.1016/S0958-9465(02)00080-X.

Consoli, N.C., Foppa, D., Festugato, L., & Heineck, K.S. (2007). Key parameters for strength control of artificially cemented soils. *Journal of Geotechnical and Geoenvironmental Engineering*, 133(2), 197-205. http://dx.doi.org/10.1061/(ASCE)1090-0241(2007)133:2(197).

Consoli, N.C., Fonseca, A.V., Silva, R.S., Cruz, R.C., & Fonini, A. (2012). Parameters controlling stiffness and strength of artificially cemented soils. *Geotechnique*, 62(2), 177-183. http://dx.doi.org/10.1680/geot.8.P.084.

Diamond, S. (1996). Delayed ettringite formation: processes and problems. *Cement and Concrete Composites*, 18(3), 205-215. http://dx.doi.org/10.1016/0958-9465(96)00017-0.

Ebailila, M., Kinuthia, J., & Oti, J. (2022). Suppression of sulfate-induced expansion with lime-silica fume blends. *Materials (Basel)*, 15(8), 2821. http://dx.doi.org/10.3390/ma15082821.

Eyo, U.E., Samuel, J.A., Samson, N., Eshmaiel, G., & Ganjian, C.E. (2021). Incorporation of a nanotechnology-based product in cementitious binders for sustainable mitigation of sulphate-induced heaving of stabilised soils. *Engineering Science and Technology. International Journal*, 24(2), 436-448. http://dx.doi.org/10.1016/j.jestch.2020.09.002.

Fonseca, A.V., Cruz, R.C., & Consoli, N.C. (2009). Strength properties of sandy soil-cement admixtures. *Geotechnical and Geological Engineering*, 27(6), 681-686. http://dx.doi.org/10.1007/s10706-009-9267-y.

He, S., Yu, X., Banerjee, A., & Puppala, A.J. (2018). Expansive soil treatment with liquid ionic soil stabilizer. *Transportation Research Record: Journal of the Transportation Research Board*, 2672(52), 185-194. http://dx.doi.org/10.1177/0361198118792996.

International Network for Acid Prevention – INAP. (2003). *Treatment of sulphate in mine effluents: lorax enviromental.* Retrieved in December 28, 2022, from www.inap.com.au

Khadka, S.D., Jayawickrama, P.W., Senadheera, S., & Segvic, B. (2020). Stabilization of highly expansive soils containing sulfate using metakaolin and fly ash based geopolymer modified with lime and gypsum. *Transportation Geotechnics*, 23, 100327. http://dx.doi.org/10.1016/j.trgeo.2020.100327.

Ladeira, A. T., & Sandoli, M. A. M. (2019). *Caracterização física, química e mineralógica de solos típicos do noroeste do Paraná para fins de aplicação em obras de pavimentação* (Projeto de iniciação científica). Maringá: Universidade Estadual de Maringá (in Portuguese).

Lens, P.N.L., Visser, A., Janssen, A.J.H., Pol, L.W.H., & Lettinga, G. (1998). Biotechnological Treatment of sulfate-rich wastewaters. *Critical Reviews in Environmental Science and Technology*, 28(1), 41-88. http://dx.doi.org/10.1080/10643389891254160.

Li, W., Yi, Y., & Puppala, A.J. (2020). Suppressing ettringite-induced swelling of gypseous soil by using magnesia-activated ground granulated blast-furnace slag. *Journal of Geotechnical and Geoenvironmental Engineering*, 146(7), 06020008-6. http://dx.doi.org/10.1061/(ASCE)GT.1943-5606.0002292.

Lukiantchuki, J.A., Oliveira, J.R.M.S., Almeida, M.S.S., Reis, J.H.C., Silva, T.B., & Guideli, L.C. (2021). Geotechnical behavior of construction waste (cw) as a partial replacement of lateritic soil in fiber-reinforced cement mixtures. *Geotechnical and Geological Engineering*, 39(2), 919-942. http://dx.doi.org/10.1007/s10706-020-01533-w.

Magalhães, J.M., Silva, J.E., Castro, F.P., & Labrincha, J.A. (2005). Physical and chemical characterisation of metal finishing industrial wastes. *Journal of Environmental Management*, 75(2), 157-166. http://dx.doi.org/10.1016/j.jenvman.2004.09.011.

Makusa, G.P. (2012). *Soil stabilization methods and materials* (Technical Report, 35 p.). Luleå: Department of Civil, Environmental and Natural Resources Engineering, Division of Mining and Geotechnical Engineering, Luleå University of Technology.

Medina, J., & Motta, L.M.G. (2015). *Mecânica dos pavimentos* (3ª ed.). Rio de Janeiro: Interciência (in Portuguese).

Mehta, P.K. (1973). Mechanism of expansion associated with ettringite formation. *Cement and Concrete Research*, 3(1), 1-6. http://dx.doi.org/10.1016/0008-8846(73)90056-2.

Mengue, E., Mrouch, H., Lancelot, L., & Eko, R.M. (2017). Physicochemical and consolidation properties of compacted lateriticsoil treated with cement. *Soil and Foundation*, 57(1), 60-79. http://dx.doi.org/10.1016/j.sandf.2017.01.005.

Mitchell, J.K. (1986). Practical problems from surprising soil behavior. *Journal of Geotechnical Engineering*, 112(3), 259-289.

Moret, A., & Rubio, J. (2003). Sulphate and molybdate ions uptake by chitin-based shrimp shells. *Minerals Engineering*, 16(8), 715-722. http://dx.doi.org/10.1016/S0892-6875(03)00169-9.

Nogami, J.S., & Villibor, D.F. (1991). Use of lateritic fine-grained soils in road pavement base courses. *Geotechnical and Geological Engineering*, 9(3-4), 167-182. http://dx.doi.org/10.1007/BF00881739.

Perrin, L.L. (1992). Expansion of lime treated clays containing sulfates. In *Proceedings of 7th International Conference on Expansive Soils*, Dallas, Texas, United States.

Portelinha, F.H.M., Lima, D.C., Fontes, M.P.F., & Carvalho, C.A.B. (2012). Modification of a lateritic soil with lime and cement: an economical alternative for flexible pavement layers. *Soils and Rocks*, 35(1), 51-63. http://dx.doi.org/10.28927/SR.351051.

Puppala, A.J., Hanchanloet, S., Jadeja, M., & Burkart, B. (1999). Evaluation of sulfate-induced heave by mineralogical and swell tests. In *Proceedings of 9th Pan-American Conference on Soil Mechanics and Geotechnical Engineering*, Santiago, Chile.

Puppala, A.J., Griffin, J.A., Hoyos, L.R., & Chomtid, S. (2004). Studies on sulfate-resistant cement stabilization methods to address sulfate-induced soil heave. *Journal of Geotechnical and Geoenvironmental Engineering*, 130(4), 391-402. http://dx.doi.org/10.1061/(ASCE)1090-0241(2004)130:4(391).

Puppala, A.J., Intharasombat, N., & Vempati, R.K. (2005). Experimental studies on ettringite-induced heaving in soils. *Journal of Geotechnical and Geoenvironmental Engineering*, 131(3), 325-337. http://dx.doi.org/10.1061/(ASCE)1090-0241(2005)131:3(325).

Santos, G.M.R., Syllos, R.S., & Benatti, C.T. (2019). Estudo da precipitação química para remoção de sulfato de efluente de anodização. In *Encontro Anual de Iniciação Científica da UEM* (p. 36). Retrieved in October 20, 2020, from http://www.eaic.uem.br/eaic2019/anais/artigos/3442.pdf

Silva, A.J., Varesche, M.B., Foresti, E., & Zaiat, M. (2002). Sulphate removal from industrial wastewater using a packed-bed anaerobic reactor. *Process Biochemistry*, 37(9), 927-935. http://dx.doi.org/10.1016/S0032-9592(01)00297-7.

Silva, A.M., Lima, R.M.F., & Leão, V.A. (2012). Mine water treatment with limestone for sulfate removal. *Journal of Hazardous Materials*, 221-222, 45-55. http://dx.doi.org/10.1016/j.jhazmat.2012.03.066.

Taylor, H.F.W., Famy, C., & Scrivener, K.L. (2001). Delayed ettringite formation. *Cement and Concrete Research*, 31(5), 683-693. http://dx.doi.org/10.1016/S0008-8846(01)00466-5.

Teixeira, P.C., Donagemma, G.K., Fontana, A., & Teixeira, W.G. (2017). *Manual de métodos de análise de solo* (3ª ed.). Brasília: Embrapa (in Portuguese).

Wang, Y.H., & Siu, W.K. (2006). Structure characteristics and mechanical properties of kaolinite soils. I. Surface charges and structural characterizations. *Canadian Geotechnical Journal*, 43(6), 587-600. http://dx.doi.org/10.1139/t06-026.

Wild, S., Abdi, M.R., & Leng Ward, G. (1993). Sulphate expansion of lime-stabilised kaolinite. Part II – Reaction products and expansion. *Clay Minerals*, 28(4), 569-583. http://dx.doi.org/10.1180/claymin.1993.028.4.07.

Wild, S., Kinuthia, J.M., Jones, G.I., & Higgins, D.D. (1999). Suppression of swelling associated with ettringite formation in lime stabilized sulphate bearing clay soils by partial substitution of lime with ground granulated blastfurnace slag. *Engineering Geology*, 51(4), 257-277. http://dx.doi.org/10.1016/S0013-7952(98)00069-6.